*J Physiol* 594.20 (2016) pp 5881–5898



The Journal of Physiology

# Age-dependent impact of $Ca_V3.2$ T-type calcium channel deletion on myogenic tone and flow-mediated vasodilatation in small arteries

Miriam F. Mikkelsen, Karl Björling and Lars Jørn Jensen

*Department of Veterinary Clinical and Animal Sciences, Faculty of Health and Medical Sciences, University of Copenhagen, Copenhagen, Denmark*

**Key points**

- Blood pressure and flow exert mechanical forces on the walls of small arteries, which are detected by the endothelial and smooth muscle cells, and lead to regulation of the diameter (basal tone) of an artery.
- $Ca_V3.2$ T-type calcium channels are expressed in the wall of small arteries, although their function remains poorly understood because of the low specificity of T-type blockers.
- We used mice deficient in $Ca_V3.2$ channels to study their role in pressure- and flow-dependent tone regulation and the possible impact of ageing on this role.
- In young mice, $Ca_V3.2$ channels oppose pressure-induced vasoconstriction and participate in endothelium-dependent, flow-mediated dilatation. These effects were not seen in mature adult mice.
- The results of the present study demonstrate an age-dependent impact of $Ca_V3.2$ T-type calcium channel deletion in rodents and suggest that the loss of $Ca_V3.2$ channel function leads to more constricted arteries, which is a risk factor for cardiovascular disease.

**Abstract** The myogenic response and flow-mediated vasodilatation are important regulators of local blood perfusion and total peripheral resistance, and are known to entail a calcium influx into vascular smooth muscle cells (VSMCs) and endothelial cells (ECs), respectively. $Ca_V3.2$ T-type calcium channels are expressed in both VSMCs and ECs of small arteries. The T-type channels are important drug targets but, as a result of the lack of specific antagonists, our understanding of the role of $Ca_V3.2$ channels in vasomotor tone at various ages is scarce. We evaluated the myogenic response, flow-mediated vasodilatation, structural remodelling and mRNA + protein expression in small mesenteric arteries from $Ca_V3.2$ knockout ($Ca_V3.2$KO) *vs.* wild-type mice at a young *vs.* mature adult age. In young mice only, deletion of $Ca_V3.2$ led to an enhanced myogenic response and a ∼50% reduction of flow-mediated vasodilatation. $Ni^{2+}$ had both $Ca_V3.2$-dependent and independent effects. No changes in mRNA expression of several important $K^+$ and $Ca^{2+}$ channel genes were induced by $Ca_V3.2$KO However, the expression of the other T-type channel isoform ($Ca_V3.1$) was reduced at the mRNA and protein level in mature adult compared to young wild-type arteries. The results of the present study demonstrate the important roles of the $Ca_V3.2$ T-type calcium channels in myogenic tone and flow-mediated vasodilatation that disappear with ageing. Because increased arterial tone is a risk factor for cardiovascular disease, we conclude that $Ca_V3.2$ channels, by modulating pressure- and flow-mediated vasomotor responses to prevent excess arterial tone, protect against cardiovascular disease.

(Received 21 August 2015; accepted after revision 18 December 2015; first published online 11 January 2016)
**Corresponding author** L. J. Jensen: Department of Veterinary Clinical and Animal Sciences, Faculty of Health and Medical Sciences, University of Copenhagen. Email: Lajj@sund.ku.dk



DOI: 10.1113/JP271470

**Abbreviations** $Ca_V3.2$KO, $Ca_V3.2$ knockout mice; CSA, cross-sectional area; EC, endothelial cell; EDH, endothelium-dependent hyperpolarization; FMVD, flow-mediated vasodilatation; $IK_{Ca}$, small conductance calcium-activated potassium channel; K9.5, Krebs buffer with 9.5 mM KCl; K75, Krebs buffer with 75 mM KCl; MR, myogenic response; MT, myogenic tone; NA, noradrenaline; NO, nitric oxide; $PGI_2$, prostacyclin; qPCR, quantitative real-time PCR; $SK_{Ca}$, intermediate conductance calcium-activated potassium channels; SMA, small mesenteric artery; SNAP, *S*-nitroso-*N*-acetyl-DL-penicillamine; TRAM-34, 1-[(2-chlorophenyl)diphenylmethyl]-1H-pyrazole; U46619, 9,11-dideoxy-11$\alpha$,9$\alpha$-epoxymethanoprostaglandin F2$\alpha$; VSMC, vascular smooth muscle cell; WT, wild-type.

## Introduction

Local regulation of blood perfusion in peripheral tissues relies in part on the mechanical forces exerted on the wall of small arteries and arterioles via changes in the intraluminal pressure (i.e. wall stress) or flow (i.e. shear stress). The myogenic response (MR) is a reflex by which an increase in pressure elicits vasoconstriction and a decrease in pressure elicits vasodilatation, such that blood flow is maintained as relatively constant throughout a broad range of pressures characteristic for each organ. Pressure is sensed by vascular smooth muscle cells (VSMCs) via mechano-sensitive proteins in the extracellular matrix coupled to membrane-spanning integrins (Hill & Meininger, 2012). Downstream myogenic depolarization, voltage-dependent $Ca^{2+}$ entry, $Ca^{2+}$ sensitization and actin polymerization are commonly considered as key events leading to acute and sustained myogenic vasoconstriction (Hill *et al.*, 2009; Walsh & Cole, 2013). Flow-mediated vasodilatation (FMVD) is initiated by an increase in lumen shear stress sensed by the endothelial cells (ECs) via a mechanism that involves $Ca^{2+}$ influx via TRPV4 channels (Kohler *et al.* 2006; Mendoza *et al.* 2010; Bubolz *et al.* 2012) and/or $P2X_4$ receptors (Yamamoto *et al.* 2000; Ando & Yamamoto, 2013). Shear stress-induced $Ca^{2+}$ entry into ECs may evoke vasodilatation via the production of vasodilators such as nitrogen oxide (NO), prostacyclin ($PGI_2$), epoxyeicosatrienoic acids and hydrogen peroxide (Bhagyalakshmi & Frangos, 1989; Fleming & Busse, 1999; Qiu *et al.* 2001; Huang *et al.* 2005; Liu *et al.* 2011). Several studies show that endothelium-dependent vasodilatation is sensitive to inhibition of the small and intermediate-conductance calcium-activated potassium channels, $SK_{Ca}$ and $IK_{Ca}$ (Shimokawa *et al.* 1996; Takamura *et al.* 1999; Brandes *et al.* 2000; Dora *et al.* 2000; Parkington *et al.* 2002; Dora *et al.* 2008; Brahler *et al.* 2009; Potocnik *et al.* 2009). Thus, an increase in EC intracellular $Ca^{2+}$ concentration ($[Ca^{2+}]_i$) to shear stress (Nilius & Droogmans, 2001) may activate $SK_{Ca}$ and $IK_{Ca}$ channels, leading to hyperpolarization of VSMCs (endothelium-dependent hyperpolarization; EDH) and vasodilatation (Miura *et al.* 2001; Si *et al.* 2006; Brahler *et al.* 2009). Accordingly, it has been suggested that the EDH mechanism plays a more prominent role in small resistance vessels than the NO-mediated pathway (Shimokawa *et al.* 1996; Brandes *et al.* 2000; Scotland *et al.* 2005; Brahler *et al.* 2009).

The family of voltage-dependent $Ca^{2+}$ channels consisting of 10 different genes is divided into the high voltage-activated channels, comprising the L-type, P/Q-type, N-type and R-type, as well as the low voltage-activated channels comprising the T-type $Ca^{2+}$ channels. The L-type channel is the major $Ca^{2+}$ entry channel coupling excitation with contraction in VSMC, and thus is of paramount importance for basal tone and blood pressure (Nelson *et al.* 1990; Smirnov & Aaronson, 1992; Moosmang *et al.* 2003). Mesenteric small arteries from rat and mouse abundantly express two of the three T-type $Ca^{2+}$ channel subtypes, namely the $Ca_V3.1$ and $Ca_V3.2$ channels (Gustafsson *et al.* 2001; Jensen *et al.* 2004; Ball *et al.* 2009; Braunstein *et al.* 2009; Björling *et al.* 2013); however, their function in the resistance vasculature remains poorly understood primarily as a result of the very low selectivity of pharmacological T-type modulators. As noted in previous studies, the T-type channels, with small unitary conductance, voltage-dependent activation/inactivation at hyperpolarized potentials and fast inactivation, may not be well suited for operating under sustained activity of VSMCs *in vivo* where the membrane potential is between –45 and –35 mV under resting physiological pressure (Perez-Reyes, 2003; Cribbs, 2006; Jensen & Holstein-Rathlou, 2009; Smirnov *et al.* 2013). This has been explained by the existence of window currents by which T-type channels can mediate basal $Ca^{2+}$ entry through a small fraction of non-inactivating channels (Bijlenga *et al.* 2000; Perez-Reyes, 2003; Jensen & Holstein-Rathlou, 2009). Furthermore, the existence of native T-type splice variants with voltage-dependent activation and inactivation curves shifted to more depolarized potentials than their recombinant counterparts may explain how $Ca^{2+}$ entry through T-type channels could have a function in arterioles (Chemin *et al.* 2001; Emerick *et al.* 2006; Jensen & Holstein-Rathlou, 2009; Kuo *et al.* 2014). A recent study addressed the significance of molecular $Ca_V3.1$ channels in vascular responses to large depolarization using high-KCl *vs.* small depolarization and stepwise increases from low to high arterial pressure. The $Ca_V3.1$ channels did not contribute to KCl- or noradrenaline (NA)-induced $Ca^{2+}$ entry or constrictions of mouse small mesenteric arteries (SMAs),

whereas, at pressures of between 20 and 80 mmHg, $Ca_V3.1$ channels were important for myogenic tone (MT) (Björling *et al.* 2013). Moreover, inhibition of $Ca_V3.2$ channels using $NiCl_2$ at micromolar concentrations did not inhibit KCl-induced $Ca^{2+}$ entry in $Ca_V3.1$ deficient mouse mesenteric arterioles in the presence of the L-type inhibitor nifedipine (Björling *et al.* 2013). Thus, in certain physiological responses or vascular beds, where the membrane potential may be rather hyperpolarized and only small changes in membrane potential occur, the T-type channels may have a distinct role compared to the L-type channels. The $Ca_V3.2$ T-type channel was shown to be expressed in VSMC and/or EC in several different resistance arteries (Blanks *et al.* 2007; Braunstein *et al.* 2009; Kuo *et al.* 2010; Poulsen *et al.* 2011), which makes the functional role of this channel particularly interesting. Because genetic ablation of the $Ca_V3.2$ T-type channel isoform leads to permanently contracted coronary arterial smooth muscle, loss of NO-mediated coronary vasodilator function and cardiac hypertrophy (with the latter being aggravated by increasing age), it appears that this isoform is involved in vasodilatation instead of vasoconstriction (Chen *et al.* 2003). The mechanism was explained to involve local $Ca^{2+}$ entry through $Ca_V3.2$ channels activating co-localized large conductance $Ca^{2+}$-activated $K^+$ channels ($BK_{Ca}$), leading to hyperpolarization of VSMC, decreased cytosolic $Ca^{2+}$ concentration and vasodilatation (Chen *et al.* 2003; Harraz *et al.* 2014*a*). To clarify the specific role of $Ca_V3.2$ channel expression in mesenteric resistance vessels, we investigated the possibility that $Ca_V3.2$ channels oppose MT and contribute to a physiological endothelium-dependent vasodilatation induced by increases in intraluminal flow. Our rigorous comparison of wild-type (WT) *vs.* $Ca_V3.2$KO mouse arteries in all experiments enabled us to test the specificity of the putative $Ca_V3.2$ inhibitor $NiCl_2$. Because there was an age-dependent effect on cardiac fibrosis in $Ca_V3.2$ deficient mice (Chen *et al.* 2003) and because ageing is normally considered to be a risk factor for high blood pressure, we also tested the effect of ageing on the role of $Ca_V3.2$ channels in MT and FMVD responses. In addition, because the prolonged loss of vasodilator function and persistent increases in vascular tone might induce structural remodelling of the arterial wall, we evaluated the passive media-to-lumen ratio and media cross-sectional area (CSA) in WT *vs.* $Ca_V3.2$KO mice in both age groups. Our results show a clear age-dependency in the contribution of $Ca_V3.2$ channels to MT and FMVD. Furthermore, $Ni^{2+}$ has both $Ca_V3.2$-dependent and independent effects. The data are discussed in the context of $Ca_V3.2$ T-type calcium channels having a specific vasodilator function in young individuals that is lost with advancing age, and we suggest that the loss of $Ca_V3.2$ channel function increases the risk for cardiovascular disease.

## Methods

### Animals and tissue preparations

Ethical approval for all animal procedures and transgenic mice were obtained from the Danish Animal Experiments Inspectorate and the Danish Working Environment Authority, respectively. $Ca_V3.2^{-/-}$ mice and age-matched C57BL/J6 WT mice in two age groups were used (young: 8–17 weeks; adult: 28–56 weeks). Homozygous $Ca_V3.2^{-/-}$ mice, originally generated by Chen *et al* (2003) were bred by mating mice heterozygous for the deletion of amino acids 216−67 in the $Ca_V3.2$ protein, and backcrossing with C57BL/J6 WT mice for at least 10 generations. Genotyping was carried out as described previously (Chen *et al.* 2003). The mice were killed by cervical dislocation and the small intestine was transferred to a petri dish with aerated (5% $CO_2$, 95% $O_2$) Krebs buffer. Sprague–Dawley rats (7–12 weeks) were anaesthetized using $CO_2$ followed by cervical dislocation. Second- or third-order branches of SMAs from mice and rats were dissected using sharpened tweezers and ophthalmic scissors under a microscope (Leica M80; Leica Microsystems, Wetzlar, Germany) and used for pressure myography, immunofluorescence microscopy and quantitative real-time PCR (qPCR).

### Pressure myography

Mouse and rat mesenteric arteries were initially relaxed in $Ca^{2+}$-free Hepes buffered PSS (mounting buffer) and mounted on two cannulas with equal-sized tips in a pressure myograph (model 120 CP; DMT A/S, Aarhus, Denmark) and then perfused with Krebs buffer to which 1% low-endotoxin BSA had been added. After mounting the vessels, the myograph chamber was continuously superfused with Krebs buffer equilibrated with 5% $CO_2$/95% $O_2$ at 37°C at a rate of 2.3 mL $min^{-1}$, thus exchanging one-third of the bath volume per minute. The vessels were viewed through a 4× objective using an inverted fluorescence microscope (Olympus IX71; Olympus Denmark A/S, Ballerup, Denmark). Lumen and vessel (outer) diameters of the arteries were measured using a USB camera and MyoView II software (both DMT A/S) on a PC. For the experiments with rats, only the outer diameter was measured as a result of a change in the software.

### Experimental protocol

Both rat and mouse mesenteric arteries were used for investigating FMVD, whereas only mouse mesenteric arteries were used for the MR. The initial mounting procedure was comparable for both types of experiment. Each experiment was divided into three trials: a control trial, an intervention and a trial using $Ca^{2+}$-free solution

with EGTA to obtain the passive/maximal diameter of the vessel. For FMVD experiments, the vessels were equilibrated at 60 mmHg for 10–15 min until the bath was 37°C with flow enabled in the pressure myograph. Initially, the vitality of the vessel was tested using Krebs buffer with high [KCl] (75 mM; K75) and, subsequently, after relaxation in Krebs, U46619 (9,11-dideoxy-11$\alpha$,9$\alpha$-epoxymethanoprostaglandin F2$\alpha$; thromboxane $A_2$ mimetic) was added directly to the bath (3.5–7 nM U46619) under no-superfusion conditions until the vessel constricted 25–50% of the resting diameter. After stable pre-constriction was obtained, flow was initiated in the same direction as the vessel had been exposed to *in vivo*, by changing the longitudinal pressure gradient ($\Delta P$) along the vessel. A $\Delta P$ of 20 mmHg at a mean intraluminal pressure of 60 mmHg was controlled by changing the pressure head by 10 mmHg in both pipettes but in opposite directions, thus creating an equal pressure drop across both pipette tips with matched resistances. In this way there is no change in pressure in the middle of the vessel (Koller *et al.* 1993). The FMVD responses measured for 3 min at $\Delta P = 20$ mmHg were reversibly induced three times in a row separated by 3 min at $\Delta P = 0$ mmHg. Following the third FMVD response, when the vessel was still constricted at $\Delta P = 0$ mmHg, the vitality of the endothelium was tested by directly adding 10 $\mu$M ACh to the bath. After resting in Krebs buffer, 30 $\mu$M $NiCl_2$ was added directly to the bath under no-superfusion conditions to inhibit the $Ca_V3.2$ $Ca^{2+}$ channels. The same procedure as used in the control trial was carried out in the presence of U46619 to obtain the same level of pre-constriction for each artery. At the end of each experiment, the vessel was superfused with $Ca^{2+}$-free Krebs buffer + EGTA to obtain the passive diameter for calculations of percentage dilatation and structural parameters. For MR experiments, the vessels were initially stretched at the maximal pressure of 120 mmHg to prevent bending, at the same time as the myograph bath was slowly heated to 37°C. In MR experiments, the luminal perfusate flow was blocked at the downstream end. The arteries were equilibrated for 15 min at 40 mmHg before initiation of the experiment. K75 was then added to constrict the vessel followed by washout with Krebs buffer, and again followed by constriction to 1 $\mu$M NA. After washout of NA, the vessels were equilibrated at 80 mmHg for 30–40 min, during which spontaneous myogenic constriction was usually observed. Next, the control pressure curve was constructed as described previously (Björling *et al.* 2013). In short, pressure was increased with an increment of 20 mmHg starting from 20 mmHg to 120 mmHg. The vessel was allowed to rest for 5 min at each step. Between the control and intervention periods, K75 was again used to constrict the vessel followed by 15 min of restitution. Subsequently, the vessel was exposed to 30 $\mu$M $NiCl_2$ for 10 min before repeating the pressure curve in the presence of $NiCl_2$. Before constructing the passive pressure curve in $Ca^{2+}$-free Krebs buffer + EGTA, the vessel was constricted to K75 in the presence of 30 $\mu$M $NiCl_2$ to test for unspecific effects of $NiCl_2$.

Vessels were excluded from further analysis in FMVD and MR experiments: (1) if the pressure in the outflow pipette dropped by >2 mmHg as a result of leaks; (2) if non-uniform constrictions of the vessel were seen; (3) if the diameter measurements were not stable or fluctuated continuously because of technical problems or vasomotion; or (4) if <40% dilatation to ACh was observed in FMVD experiments.

### Immunofluorescence microscopy

Immunostaining and fluorescence microscopy was performed as described previously (Björling *et al.* 2013). In brief, mouse mesenteric arteries were dissected, fixated for 15 min in 2% paraformaldehyde in PBS and subsequently kept in 30% sucrose in PBS for 1 h before they were snap-frozen in liquid nitrogen when embedded in Tissue-Tek® (Sakura Finetek Denmark Aps, Denmark). Frozen sections (5 $\mu$M) of the vessels were cut using a Cryostat (Leica CM 1950) and subsequently transferred to SuperFrost Plus microscope slides (Thermo Scientific, Fisher Scientific GmbH, Germany) where they were treated as described previously (Björling *et al.* 2013). A polyclonal antibody raised in rabbit against an epitope of the $Ca_V3.2$ T-type $Ca^{2+}$ channel (anti-$Ca_V3.2$, Alomone Labs, Jerusalem, Israel) was diluted 1:100 or 1:200 in PBS and applied to the sections. Peptide pre-incubation controls were included for $Ca_V3.2$ Alomone antibody using its short epitopic peptide as described previously for rats (Braunstein *et al.* 2009). In some WT vessels, we also tested the intensity of $Ca_V3.1$ T-type channel staining, using a $Ca_V3.1$ antibody (1:1500) kindly provided by Dr Leanne Cribbs (Loyola University, IL, USA) and characterized previously (Björling *et al.* 2013; Brueggemann *et al.* 2005). After treatment with primary and secondary antibodies (dilution 1:800; Donkey anti-rabbit Alexa Fluor 594) and 4′,6-diamidino-2-phenylindole (dilution 1:10.000; both Life Technologies, Grand Island, NY, USA), a cover slip was mounted using anti-fade medium (Dako, Glostrup, Denmark ). A BX50 fluorescence microscope (Olympus) equipped with a UPlanApo 40×/1.00 oil iris high-quality quartz objective was used for inspection and images were acquired using a Retiga 6000 cooled monochrome CCD camera and Q-Capture Pro7 software (Q-Imaging Inc., Surrey, BC, Canada). All images were acquired using the exact same camera settings and the same type of final adjustments were applied using Photoshop CS6 (Adobe Systems Inc., San Jose, CA, USA). Background-corrected total tissue fluorescence of $Ca_V3.1$-specific staining was quantitated using ImageJ, version 1.48 (NIH, Bethesda, MD, USA) and compared in images acquired using

**Table 1. Primer sets used in qPCR**

| Gene name | Forward primer (5′- 3′) | Reverse primer (5′- 3′) | Product size (bp) | Accession number |
|---|---|---|---|---|
| Kcnma1 | CAGTTTGACCACAACGCTGG | TGTGGGTACTCATGGGCTTG | 233 | NM001253378 |
| Kcnmb1 | CTCAACAGGTCCCTATCCATCT | CCAAAGTCACTGGGAATCGGA | 200 | NM031169 |
| Cacna1c | CGTTCTCATCCTGCTCAACA | GGTGTACCTCGGTGATTGCT | 236 | BC138031 |
| Cacna1g | TCATAGCCGTGCTGATGAAG | AAGGGAGAAGCCTGAAGAGG | 236 | NM009783.3 |
| Cacna1h | CCTTTCTCAGCGTCTCCAAC | GCCACAATGATGTCAACCAG | 169 | BC138026 |
| Cacna1a | TGCTGTGCTCACTGTTTTCC | TTCTCCACACGTTCCCTTTC | 198 | NM007578 |
| Trpc1 | GACATTCCAGGTTTCGTCTTG | GTCAGCACTAAGTTCAAACGC | 107 | NM011643 |
| Trpc3 | GATCGAGGATGACAGTGATGTAG | TCCATCATCGAAGTAGGAGAGC | 73 | NM019510 |
| Trpc6 | TACAATCTGGCCAGGATAAAGTG | CACAGCGATTGCATAAAGACC | 75 | NM013838 |
| Actb | AGCCATGTACGTAGCCATCC | CTCTCAGCTGTGGTGGTGAA | 228 | NM007393 |

simultaneous incubations of young and adult SMAs and the same settings of the fluorescence microscope and CCD camera.

### qPCR

Second- and third-order branches of both young and adult mouse mesenteric arteries were stored until use in RNAlater (Thermo Scientific) at 4°C. Endothelial tubes were isolated from 1–3 mm long segments of young mouse SMAs as described previously for mouse superior epigastric arteries (Socha & Segal, 2013). However, the SMA incubation time with collagenase (1.5 mg $mL^{-1}$) + papain (0.62 mg $mL^{-1}$) + 1,4-dithioerythritol (1 mg $mL^{-1}$) in dispersion buffer was increased to 60–70 min at 37°C to facilitate rapid isolation of endothelial tubes without scattered remaining VSMCs. Ten endothelial tubes from each mouse were transferred directly to the homogenization buffer. Tissue homogenization and extraction of RNA were performed as described previously using TissueLyzer and a RNEasy Micro kit (Qiagen, Hildenberg, Germany) (Björling *et al.* 2013). Subsequently, cDNA was made using a kit obtained from Promega (Madison, WI, USA) in accordance with the manufacturer's instructions. RT+ and RT– samples were prepared. Primer sets used are shown in Table 1. qPCR was performed using LightCycler 480 (Roche Diagnostics A/S, Hvidovre, Denmark) and SYBR Green PCR Master Mix (Qiagen). The qPCR protocol comprised annealing at 60°C for 10 s and elongation at 72°C for 20 s. Efficiencies were in the range 1.83–1.98 and slopes in the range –3.34 to –3.67. Melting curve analysis showed only single peaks. Samples with $H_2O$ or RT– did not show any product or the product appeared at least 10 cycles later than for RT+ samples. Expression of $\beta$-actin (i.e. the reference gene) did not vary significantly between samples.

### Solutions and chemicals

Krebs buffer (in mM): 118 NaCl, 4.7 KCl, 1.2 $MgSO_4$, 2 $CaCl_2$, 25 $NaHCO_3$ and 1.2 $KH_2PO_4$. $Ca^{2+}$-free solution for passive diameter measurements was prepared as described for Krebs buffer, except that $CaCl_2$ was replaced by 2 mM EGTA. In Krebs buffer with 9.5 or 75 mM KCl, the additional amount of $K^+$ replaced equimolar amounts of $Na^+$. $Ca^{2+}$-free Hepes-buffered PSS (mounting buffer; in mM): 140 NaCl, 5 KCl, 1.2 $MgSO_4$ and 10 Hepes, with the pH being adjusted to 7.4 with NaOH. Note that 5 mM glucose was added to the above-mentioned buffers before use. Dissection buffer for endothelial tube isolation was $Ca^{2+}$-free Hepes-buffered PSS with 10 mM glucose and 0.1% BSA added. The dissociation buffer for endothelial tube isolation was Hepes-buffered PSS with 2 mM $CaCl_2$ + 10 mM glucose + 0.1% BSA. The pH of all solutions except the PSS buffers was adjusted continuously by equilibration with 5% $CO_2$/95% $O_2$. Low-endotoxin BSA, $NiCl_2$, U46619, NA, apamin, 1-[(2-chlorophenyl)diphenylmethyl]-1H-pyrazole (TRAM-34), L-NAME, *S*-nitroso-*N*-acetyl-DL-penicillamine (SNAP), paxilline, collagenase, papain, 1,4-dithioerythritol and chemicals of reagent grade were obtained from Sigma-Aldrich (St Louis, MO, USA), unless stated otherwise.

## Statistical analysis

Percentage of dilatation in the FMVD, ACh, SNAP and Krebs buffer with 9.5 mM KCl (K9.5) experiments was calculated as:

$$\%\ \text{dilatation} = \frac{\Delta D}{\Delta D_{\max}} \times 100 = \frac{D - D_{\text{baseline}}}{D_{\max} - D_{\text{baseline}}} \times 100$$

where $D_{\text{baseline}}$ is the diameter when pre-constricted with U46619, $D$ is the peak diameter measured at $\Delta P = 20$ mmHg or with ACh, SNAP or K9.5, and $D_{\max}$ is the diameter in $Ca^{2+}$-free Krebs' buffer + EGTA.

The MT was calculated as the percentage difference in active lumen diameter in Krebs buffer and in $Ca^{2+}$-free Krebs buffer + EGTA at each pressure step using:

$$\%\ \text{myogenic tone} = \frac{D_{Ca^{2+}\text{free KB}} - D_{\text{KB}}}{D_{Ca^{2+}\text{free KB}}} \times 100$$

Statistical testing of differences between mouse genotypes within age-groups was performed using two-way ANOVA with a Bonferroni *post hoc* test for pairwise comparison of the MR and SNAP data. Student's *t* test was used for comparison of dilatations to flow, ACh and K9.5 between genotypes. One-way ANOVA with the Bonferroni *post hoc* test was used for comparison of the effects of genotype and age for the structural remodelling and vasoconstrictor effects of K75 and NA. A Kruskal–Wallis test with Dunn's *post hoc* test was used for comparison of mRNA expression across genotype and age. $P < 0.05$ was considered statistically significant.

## Results

### MR

Because a previous study reported that the coronary arteries of $Ca_V3.2$ deficient mice ($Ca_V3.2$KO) were chronically more contracted than their matching WT mice (Chen *et al.* 2003), we hypothesized that the MR and MT would be enhanced in $Ca_V3.2$KO. We first tested, in SMAs from young WT mice (8–15 weeks), the effect on MR of a low concentration of $NiCl_2$ (30 $\mu$M) considered to be specific for $Ca_V3.2$ channels (Lee *et al.* 1999). The active curve in Fig. 1*A* shows that a MR was elicited at pressures >60 mmHg in contrast to the passive distension of the vessels shown in the passive curve. However, the presence of 30 $\mu$M $NiCl_2$ caused the SMAs to be significantly more constricted than the active curve in the pressure range 40–100 mmHg. Next, we employed SMAs from young $Ca_V3.2$KO mice (8–15 weeks) to test the validity of this finding. As shown in Fig. 1*B*, the active curve is more constricted throughout the pressure range tested and there was no significant effect of adding 30 $\mu$M $NiCl_2$. At low pressure (20-40 mmHg), the $NiCl_2$-treated $Ca_V3.2$KO vessels were somewhat more constricted than the active curve, although this was not significant. Nevertheless, it could indicate a $Ca_V3.2$ independent effect of $NiCl_2$. Because ageing in humans is associated with stiffening of major arteries and an increase in systolic blood pressure, we decided to test the above effects in older mice. When we tested the MR in adult, middle-aged WT mice (32–56 weeks), we observed active constriction at pressures >40 mmHg and generally more constriction of SMAs than in young mice (Fig. 1*C*), and there was no significant effect as a result of adding 30 $\mu$M $NiCl_2$. When we tested this in age-matched $Ca_V3.2$KO mice, we observed a pattern similar to that in WT mice (i.e. the active curve shows constriction at pressures >40 mmHg), with no additional effect of adding $NiCl_2$ (Fig. 1*D*). Thus, the impact of $Ca_V3.2$ deletion with respect to enhancing MT in young mice (Fig. 1*E*) is not present in mature adult (middle-aged) mice (Fig. 1*F*). Using $NiCl_2$ as a tool, the results of the original study by Chen *et al.* (2003) and a recent study by Harraz *et al.* (2014*a*) suggested that $Ca_V3.2$ channels and $BK_{Ca}$ channels in arterial myocytes are functionally coupled to promote vasodilatation. To tests this hypothesis with our knockout model, we repeated the MR experiments in young mice in the presence of 1 $\mu$M paxilline (a specific blocker of $BK_{Ca}$ channels). We found that the MT curves were significantly different before and after the addition of paxilline in young WT mice (Fig. 1*G*), whereas no significant effect was seen in $Ca_V3.2$ knockout ($Ca_V3.2$KO) mice (Fig. 1*F*). These data demonstrate that an interaction between $Ca_V3.2$ channels and $BK_{Ca}$ channels at the level of individual VSMCs is possible.

### KCl- and NA-induced vasoconstriction

To complete our characterization of the contractile properties of the VSMC in SMA of $Ca_V3.2$KO and WT mice, we also performed tests of electromechanical and neurohormonal vasoconstriction using high-KCl (75 mM) and NA (1 $\mu$M). These responses were evaluated as the percentage increase in vascular tone ($\Delta$Tone) upon exposure to the stimulus and are shown in Table 2. There were no differences between KCl-induced vasoconstriction between WT and $Ca_V3.2$KO in young mice or adult mice. Furthermore, there were no significant effects on KCl-induced responses to the addition of 30 $\mu$M $NiCl_2$. For NA responses, no differences were detected between WT and $Ca_V3.2$KO mice in either of the two age groups; however, we observed a statistically significant increase in percentage tone in adult *vs.* young WT mice. Accordingly, we found a main effect of ageing with respect to increasing KCl- and NA-induced vasoconstriction ($P < 0.01$ and $P < 0.001$, respectively) when including all mice in the analysis.

### FMVD

Because increased basal tone in $Ca_V3.2$KO mice could also be a result of endothelial dysfunction, we decided to test the vasodilator response to an increase in shear stress, which is a physiologically important stimulator of endothelium-dependent vasodilatation. First, we established a protocol for measuring FMVD responses in the pressure myograph. We initially used rat SMAs because $Ca_V3.2$ channels were previously shown to be expressed in ECs of rat SMAs and arterioles (Braunstein *et al.* 2009) and because FMVD has previously been measured in this vascular bed (Thorsgaard *et al.* 2003;Christensen *et al.* 2007). Figure 2A shows an original recording in which a reversible FMVD response in a pre-constricted SMA was elicited at a mean pressure of 60 mmHg to flow/shear stress induced by a longitudinal pressure gradient of 20 mmHg. When rat SMAs were exposed to the NOS inhibitor L-Name (100 $\mu$M), no significant inhibition

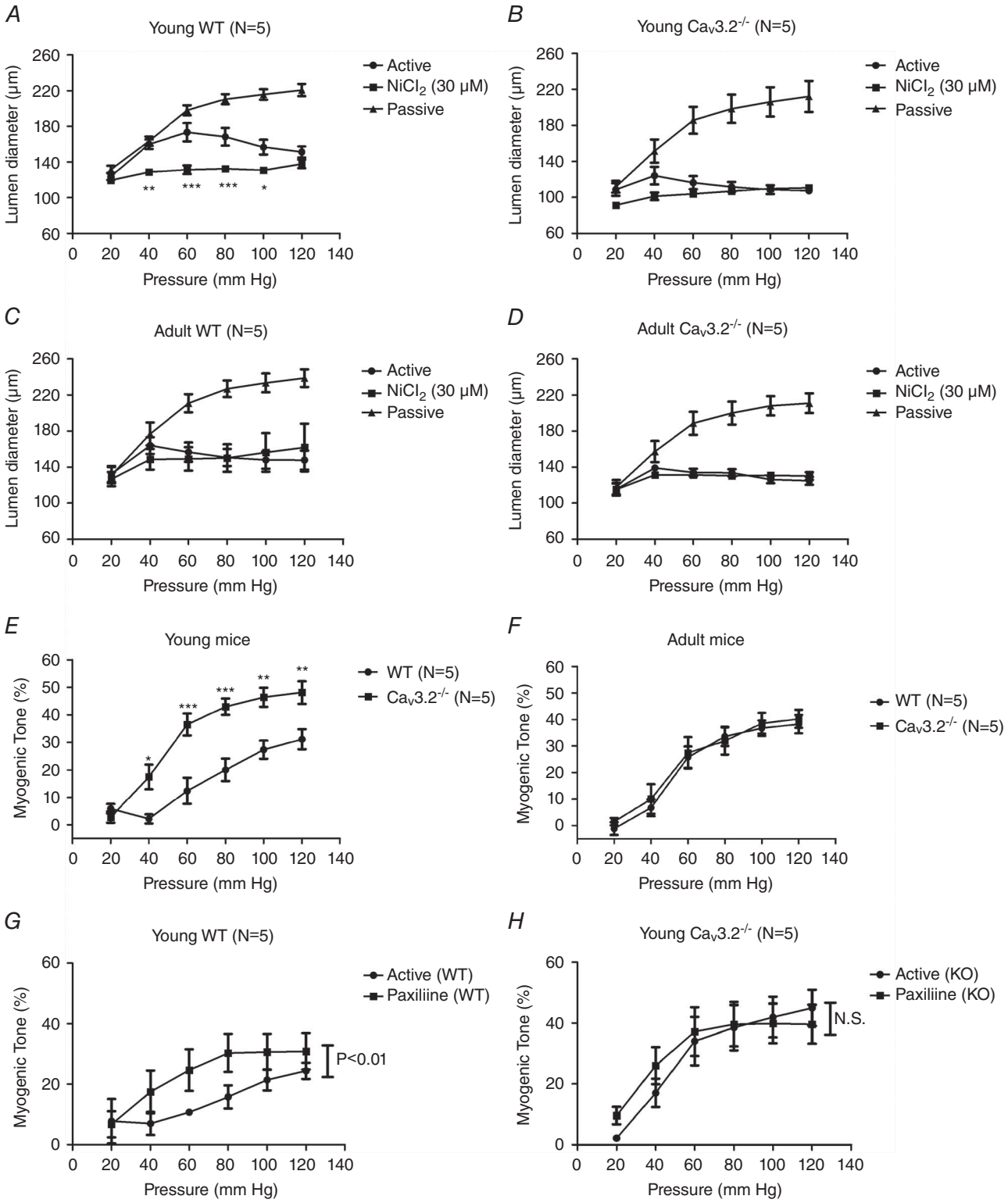


**Figure 1. Myogenic responsiveness in young *vs.* mature WT and $Ca_V3.2$KO mice**
Myogenic response (and effects of 30 $\mu$M $Ni^{2+}$) in young WT (*A*), young $Ca_V3.2$KO (*B*), mature adult WT (*C*) and mature adult $Ca_V3.2$KO (*D*) mouse mesenteric artery. Myogenic tone (MT, %) in young WT *vs.* $Ca_V3.2$KO mice (*E*, same mice as in *A* and *B*), and mature adult WT *vs.* $Ca_V3.2$KO mice (*F*, same mice as in *C* and *D*). Effects of paxilline on MT in young WT (*G*) *vs.* $Ca_V3.2$KO mice (*H*). $^*P < 0.05$; $^{**}P < 0.01$; $^{***}P < 0.001$ at individual pressures.

**Table 2. KCl- and NA-induced vasoconstriction in mouse SMAs**

| Delta tone (%) | Young WT ($n = 5$) (8–17 weeks) | Adult WT ($n = 5$) (28–56 weeks) | Young KO ($n = 5$) (8–17 weeks) | Adult KO ($n = 5$) (28–56 weeks) |
|---|---|---|---|---|
| KCl (75 mM) | 74.6 ± 3.7 | 87.5 ± 4.4 | 70.0 ± 4.5 | 87.4 ± 4.8 |
| KCl + $NiCl_2$ (30 $\mu$M) | 61.9 ± 3.6 | 64.6 ± 13.8 | 59.6 ± 6.1 | 81.2 ± 5.5 |
| NA (1 $\mu$M) | 22.8 ± 4.0 | 47.0 ± 6.6* | 30.1 ± 5.7 | 49.5 ± 5.9 |

*$P < 0.05$ *vs.* young WT.

of FMVD was observed (Fig. 2*B*). In a parallel set of experiments, incubation for 30–40 min with the $SK_{Ca}$ $Ca^{2+}$-activated $K^+$ channel blocker apamin (50 nM) and the $IK_{Ca}$ channel blocker Tram-34 (1 $\mu$M) almost abolished the FMVD responses in rat SMAs (Fig. 2*C*). In preliminary experiments, we could not detect any effects of incubation with indomethacin and, indeed, previous studies have shown potent FMVD responses in the presence of this drug in rat SMAs (Thorsgaard *et al.* 2003; Christensen *et al.* 2007). Next, we tested the effect of 100 $\mu$M $NiCl_2$ with respect to blocking the $Ca_V3.2$ channels and, unexpectedly, we found that the dilatation induced by intraluminal flow was converted to a constriction (Fig. 2*D*). We speculated that this reversal of the response could partially be the result of an unspecific effect of $NiCl_2$ and we therefore aimed to test the hypothesis that endothelial $Ca_V3.2$ channels is part of the mechanism in the FMVD response using WT *vs.* $Ca_V3.2$KO mice. In WT mice, the percentage dilatation to flow was less than in rats (compare Figs 2 and 3), whereas the FMVD response was significantly reduced in young $Ca_V3.2$KO mice compared to young WT mice (Fig. 3*A*). In young WT and $Ca_V3.2$KO mice, the effect of 30 $\mu$M $NiCl_2$ ($IC_{50} = 12$ $\mu$M for $Ca_V3.2$) (Lee *et al,* 1999) was not significant, although there was an apparent reversal of FMVD to a constriction in young $Ca_V3.2$KO mice. We also investigated FMVD in mature adult mice, and we found no significant difference between the groups (Fig. 3*B*). When the main effect of $NiCl_2$ was tested in all mice (both genotypes, both ages), there was a significant reduction in FMVD in the presence of $NiCl_2$

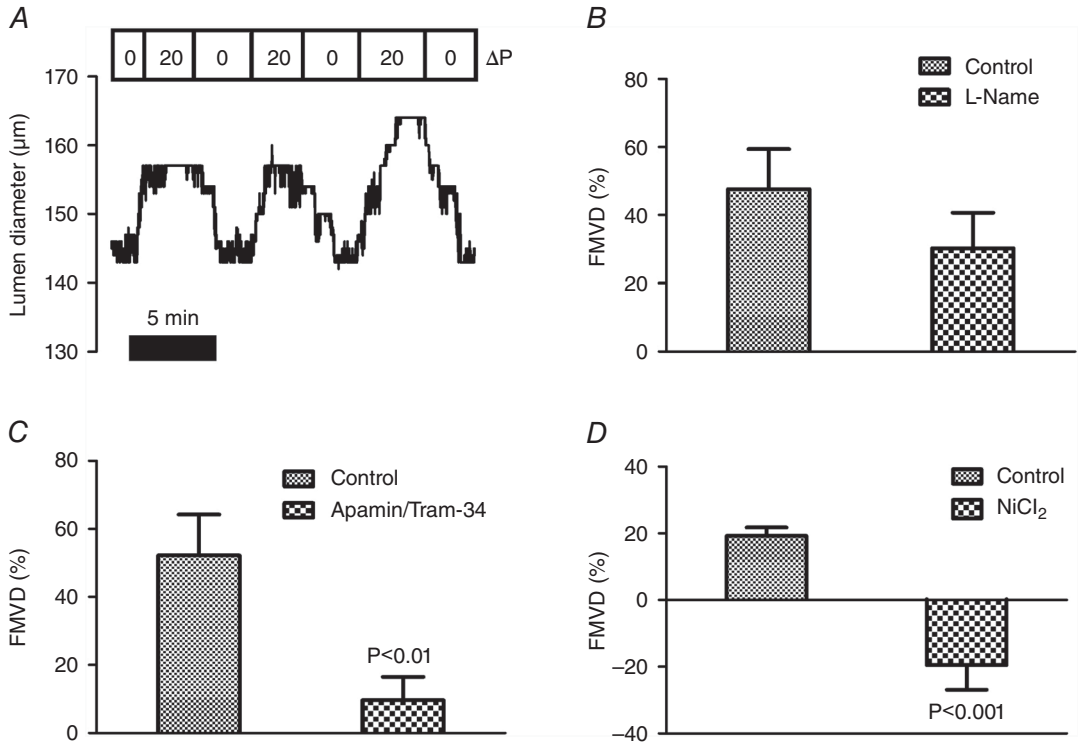


**Figure 2. Flow-mediated vasodilatation in rat small arteries**
Original recording showing reversibility of FMVD (%) in SMAs induced by a longitudinal pressure gradient ($\Delta P = 20$ mmHg) at a mean pressure of 60 mmHg in a cannulated vessel preconstricted using U46619 (*A*). Effects of L-Name (100 $\mu$M) (*B*); apamin (50 nM) + Tram-34 (1 $\mu$M) (*C*); and $NiCl_2$ (100 $\mu$M) (*D*) on FMVD responses in rat mesenteric artery.

($P < 0.05$; $n = 29$–30). These data appear to suggest that $NiCl_2$ exerted effects that were not mediated solely by $Ca_V3.2$ channel inhibition. There was no difference in FMVD between the young and adult WT mice, nor between the young and adult $Ca_V3.2$KO mice. There was also no difference when age as a main effect was tested.

### ACh-induced vasodilatation

In pressurized (60 mmHg), pre-constricted (U46619) mouse SMAs, we tested the capacity for full endothelium-dependent vasodilatation by adding a high concentration (10 $\mu$M) of ACh to the pressure myograph bath. In young WT mice, ACh induced an ~70% vasodilatation, which was partially blocked by the addition of 30 $\mu$M $NiCl_2$ (Fig. 4*A*, left). In young $Ca_V3.2$KO, we observed an ~80% ACh-dilatation, which was not significantly different from WT. Again, $NiCl_2$ induced block of ACh-dilatation (Fig. 4*A*, right). When we tested the same experimental conditions in adult WT and $Ca_V3.2$KO mice, we observed results that were qualitatively and quantitatively similar to those obtained in the young mice (Fig. 4*B*). Thus, the effect of $NiCl_2$ on ACh-dilatation in pressurized mouse SMAs was not caused by $Ca_V3.2$ channels, which appears to support the unspecific role of $NiCl_2$, as suggested by the FMVD results reported above.

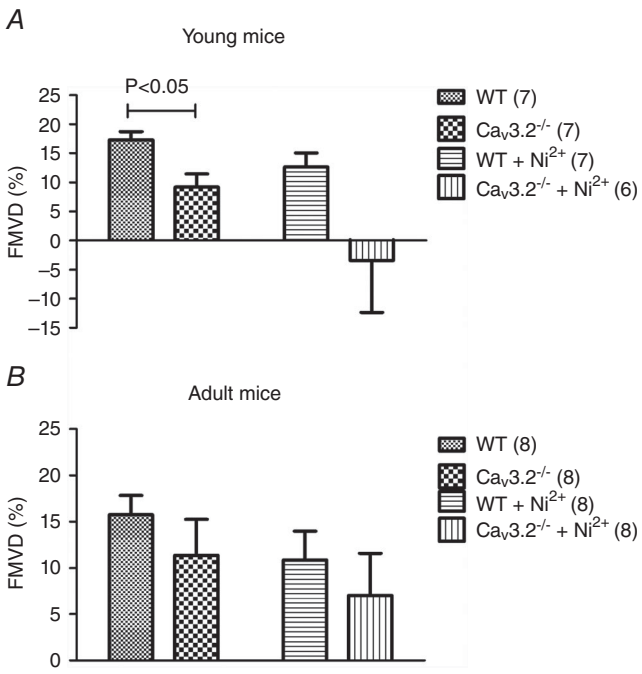


**Figure 3. FMVD measurements in WT *vs.* $Ca_V3.2$KO mice**
FMVD (and effects of 30 $\mu$M $Ni^{2+}$) in young WT *vs.* $Ca_V3.2$KO mouse mesenteric arteries (*A*) and in mature adult WT *vs.* $Ca_V3.2$KO arteries (*B*).

### Endothelium independent vasodilatation

Because T-type channel activity has been shown to be regulated by cGMP/PKG (Harraz *et al.* 2014*b*) downstream of NO release, we decided to circumvent EC activation and to test the effect of activating the cGMP/PKG pathway in VSMC using the specific and potent NO-donor SNAP. In concentrations from $10^{-7}$ to $10^{-5}$ M, we observed a highly similar degree of vasodilatation in pressurized, pre-constricted mouse SMAs from WT *vs.* age-matched $Ca_V3.2$KO mice (Fig. 4*C*). Because $Ca_V3.2$ channels are more active at hyperpolarized membrane potentials, we tested the vasodilatation to a moderate elevation of bath [KCl] (to 9.5 mM), which is known to activate $K_{IR}$ channels and Na/K-ATPase and also cause hyperpolarization of VSMCs and vasodilatation (Edwards *et al.*, 1998). However, exposure of pressurized, pre-constricted mouse SMAs to 9.5 mM $K^+$ in Krebs buffer resulted in a highly similar degree of vasodilatation in WT and age-matched $Ca_V3.2$KO mice (Fig. 4*D*). We did not test the effects of $NiCl_2$ in these experiments. These data clearly demonstrate that $Ca_V3.2$ channels do not participate in endothelium independent vasodilatation.

### Acute effects of $Ni^{2+}$ on resting diameter

The possible contribution of $Ca_V3.2$ channels to baseline diameter at an *in vivo*-like intravascular pressure of 60 mmHg was evaluated as the absolute constrictions seen directly after $NiCl_2$ addition to the myograph bath. As shown in Fig. 5, there was a constriction in young WT mice upon acute exposure to 30 $\mu$M $NiCl_2$, and a similar significant effect was seen in age-matched $Ca_V3.2$KO mice. Qualitatively and quantitatively similar results were obtained with the same protocol in adult WT mice and age-matched $Ca_V3.2$KO mice. These data clearly demonstrate that, in pressurized resistance vessels, $Ni^{2+}$ cannot be used as a specific blocker of $Ca_V3.2$ channels even at this low concentration.

### Structural remodelling of the vascular wall

Because both calcium and ageing are known to play a role in remodelling processes in the vascular wall, we tested the passive structural properties of the arterial wall in SMAs from young and adult WT and $Ca_V3.2$KO mice. We evaluated passive lumen diameter, passive vessel (outer) diameter, passive wall thickness, passive media/lumen-ratio and passive media CSA at 60 mmHg. Fig. 6 shows the data obtained for passive lumen diameter, media/lumen-ratio and media CSA only. Overall, there were no statistical differences between the WT and $Ca_V3.2$KO arteries in either young or mature adult mice. However, in arteries from both WT and $Ca_V3.2$KO mice, we found a main effect of age on passive media CSA, which

was significantly increased in mature adult mice ($P < 0.05$; $n = 24$–26) (Fig. 6*C*).

## $Ca_V3.2$ localization

In a previous study using immunofluorescence microscopy, we reported the expression of $Ca_V3.2$ protein in both vascular smooth muscle and endothelium in rat SMAs and arterioles (Braunstein *et al.* 2009). In SMAs from young mice ($n = 3$), we found a homogeneous distribution of red $Ca_V3.2$ fluorescence in the media layer of the vessels corresponding to abundant $Ca_V3.2$ expression in VSMCs. A faint red staining corresponding to a weak $Ca_V3.2$ expression is seen in the intima layer next to EC nuclei on the lumen side of the green autofluorescent internal elastic lamina (Fig. 7*A*). In the peptide pre-incubation control (Fig. 7*B*), we did not observe any red fluorescence, thus clearly demonstrating the specificity of the antibody. We also compared the $Ca_V3.2$ staining in young ($n = 2$) *vs.* adult ($n = 2$) mesenteric arteries and found no difference in the staining pattern or intensity (data not shown). Finally, we tested the mRNA expression of Cacna1H by qPCR on ∼10 isolated endothelial tubes (Fig. 7*C*) from each of four young WT mice. In these experiments, crossing point ($C_t$) values in the range 35–40 cycles for Cacna1H indicated a low

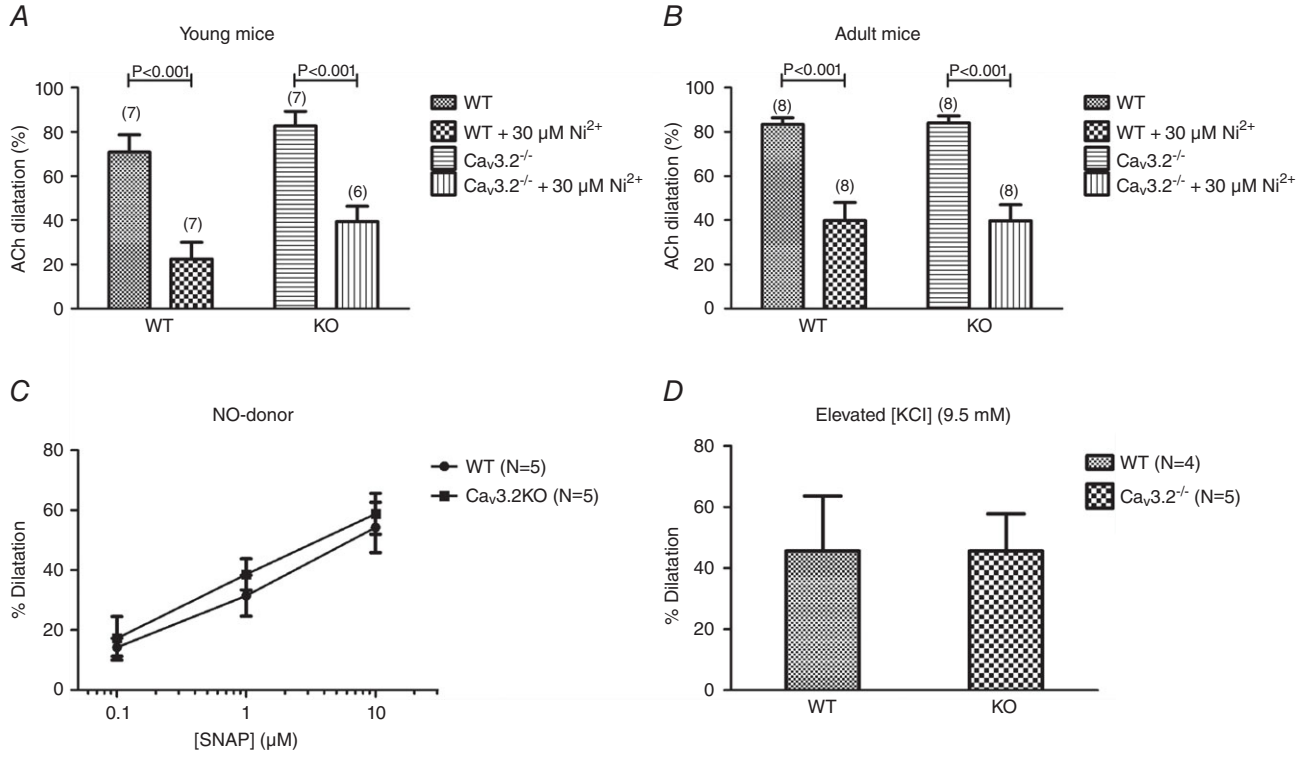


**Figure 4. Endothelium-dependent (*A, B*) and - independent (*C, D*) vasodilatation in WT *vs.* $Ca_V3.2$KO mice**
Dilatations (%) to ACh (ACh, 10 $\mu$M) in young WT *vs.* $Ca_V3.2$KO mouse mesenteric arteries (*A*) and in mature adult WT *vs.* $Ca_V3.2$KO arteries (*B*). *C*, concentration-dependent dilatations to NO-donor SNAP in age-matched WT *vs.* $Ca_V3.2$KO arteries. *D*, dilatations to elevated bath [KCl] = 9.5 mM in age-matched WT *vs.* $Ca_V3.2$KO arteries.

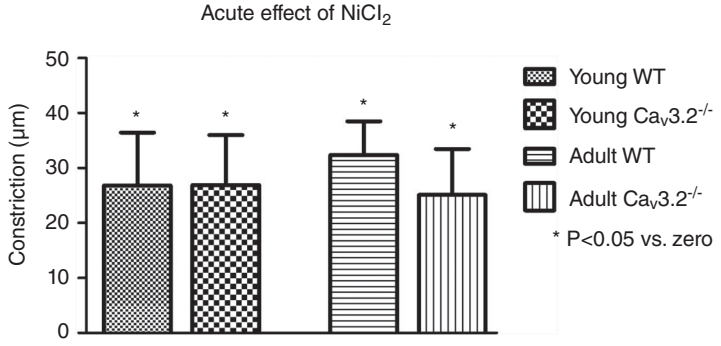


**Figure 5. Acute vasoconstriction to $NiCl_2$**
Acute vasoconstriction upon exposure to 30 $\mu$M $NiCl_2$ in pressurized (60 mmHg) mesenteric arteries in young WT *vs.* $Ca_V3.2$KO arteries and in mature adult WT *vs.* $Ca_V3.2$KO arteries.

gene expression level in endothelial tubes. ActB gene ($\beta$-actin) was consistently amplified in all endothelial samples, with $C_t$ values in the range 25–29 cycles (data not shown). The gel in Fig. 7*D* shows bands for the qPCR using Cacna1H primers in endothelial tubes (EC1–EC4) corresponding to the correct Cacna1H product size of 169 bp. To check for contamination with VSMCs in our qPCR using endothelial tubes, we quantitated gene expression of Cacna1C (L-type channel) in these four mice; however, this was found to be negative, confirming the purity of our endothelial tube isolation (data not shown). Thus, transcription of Cacna1H into mRNA appears to occur at a low level in ECs, which is only barely detectable as translated protein expression in the endothelium of mouse mesenteric arteries *in situ*.

### $Ca^{2+}$ and $K^+$ channel expression profile

Because we have compared four different groups of mice (young WT, young knockout, adult WT, adult knockout), we investigated the level of expression of several $Ca^{2+}$ channel and $K^+$ channel genes in SMAs to check for transcriptional changes that could potentially interfere with our conclusions. As shown in Table 3, we did not find any significant differences between the four groups with respect to the expression of the $BK_{Ca}$ $\alpha_1$- and $\beta_1$-subunits, $Ca_V1.2$, $Ca_V2.1$, $Ca_V3.2$ (using WT, only), TRPC1, TRPC3 or TRPC6. Surprisingly, for $Ca_V3.1$, we found a highly significant down-regulation of mRNA expression in adult WT SMA compared to young WT, whereas only a tendency for the same change was observed between young *vs.* adult $Ca_V3.2$KO mice. To check the relevance of this dramatic difference (>50%) in $Ca_V3.1$ mRNA, we tested the hypothesis that it should be visible in immunostaining experiments. We therefore performed immunofluorescence microscopy using a previously characterized $Ca_V3.1$ antibody (Björling *et al.* 2013; Brueggemann *et al.* 2005) and found much brighter fluorescence in SMAs from young (Fig. 8*A*) compared to adult SMAs (Fig. 8*B*). When we measured the arbitrary fluorescence intensity corrected for background fluorescence and normalized it to the area of the tissue examined, we observed a lower intensity in the adult SMAs (Fig. 8*D*). We performed similar measurements in SMAs from $Ca_V3.2$ KO mice

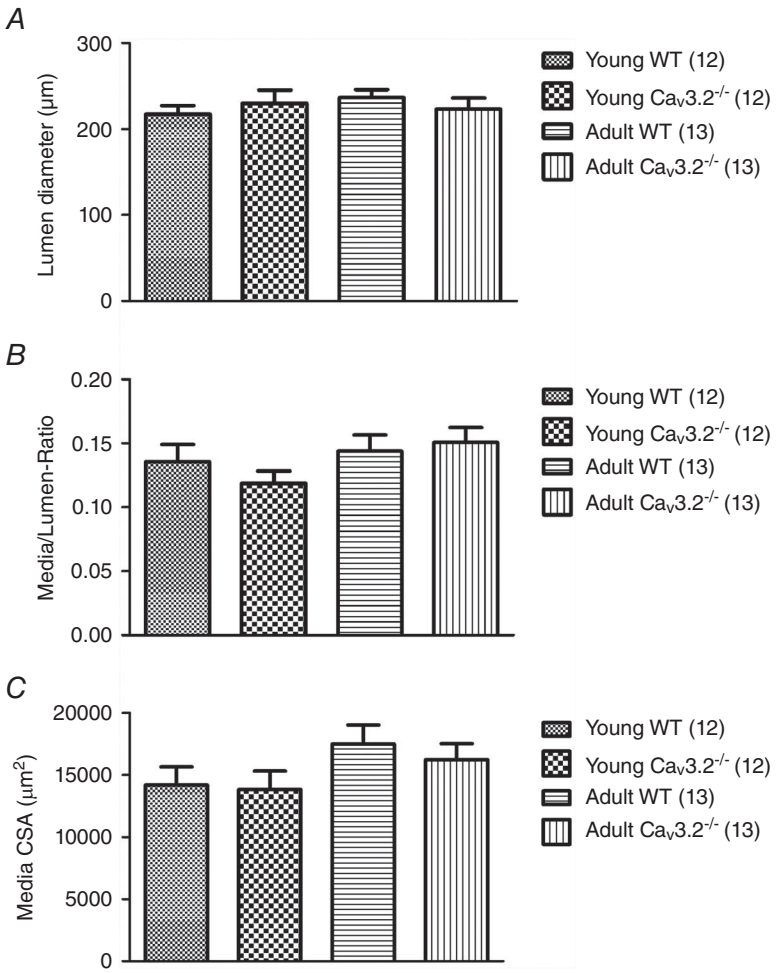


**Figure 6. Passive structural properties of SMAs**
Passive lumen diameter (*A*), media/lumen-ratio (*B*) and media CSA (*C*) in WT *vs.* $Ca_V3.2$KO arteries for both young and mature adult mice.

aged 2 months (young; 4 vessels in one mouse), 8 months (adult; 7 vessels in 2 mice) and 21 months (old; 7 vessels in 2 mice) but we did not observe any difference in the staining intensity between these age groups (data not shown). Thus, these findings are consistent with an age-dependent transcriptional down-regulation of $Ca_V3.1$ channels in WT mice detectable at the mRNA and protein levels.

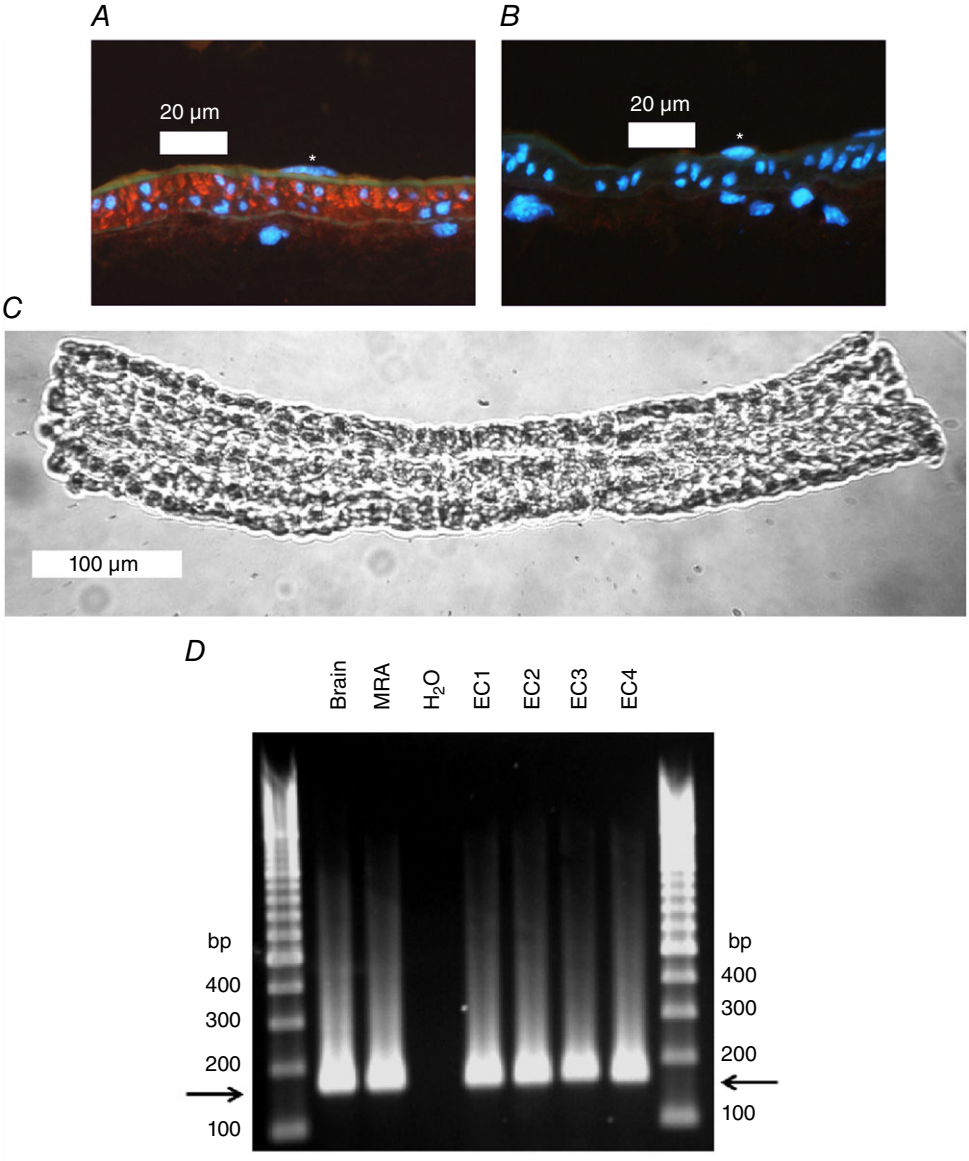


**Figure 7. Expression of $Ca_V3.2$ at the mRNA and protein level in young mouse SMAs**
*A*, mouse SMA (young) stained with primary antibody against $Ca_V3.2$ (red colour). The internal and external elastic laminas are visible as faint green bands using the inherent autofluorescence of the tissue. Nuclei are stained blue with 4′,6-diamidino-2-phenylindole. An endothelial cell nucleus is marked with an asterisk in the vessel lumen. Clear $Ca_V3.2$-specific red staining is present in the media layer and faint red staining is visible in the intima layer on the luminal side of the green internal elastic lamina. *B*, negative peptide pre-absorption control staining for $Ca_V3.2$ primary antibody of mouse mesenteric artery (young). Note the absence of a positive red signal. An endothelial cell nucleus is marked with an asterisk in the vessel lumen. *C*, image of isolated endothelial tube from a young mouse SMA. The image was acquired with a Axiovert S-100 microscope (Carl Zeiss, Oberkochen, Germany) through a Neofluar 20× objective using a USB camera and Myoview II software. *D*, agarose gel showing electrophoresis of Cacna1H qPCR products from mouse brain ($n = 1$), mouse whole SMA ($n = 1$) and SMA endothelial tubes isolated from four young WT mice (EC1–EC4). Horizontal arrows depict the product size corresponding to Cacna1H (169 bp). Note the similar product size in brain, whole SMA and EC tubes.

**Table 3. mRNA expression of selected ion channels in mouse sMAs**

| Gene name (protein name) | Young WT (8–17 weeks) | Adult WT (28–56 weeks) | Young KO (8–17 weeks) | Adult KO (28–56 weeks) |
|---|---|---|---|---|
| Kcnma1 ($BK_{Ca}$ $\alpha_1$) | 0.036 ± 0.002 | 0.040 ± 0.005 | 0.032 ± 0.004 | 0.035 ± 0.003 |
| Kcnmb1 ($BK_{Ca}$ $\beta_1$) | 19.35 ± 0.63 | 20.84 ± 0.70 | 15.96 ± 1.14 | 18.98 ± 0.42 |
| Cacna1c ($Ca_V1.2$) | 0.241 ± 0.012 | 0.286 ± 0.020 | 0.235 ± 0.025 | 0.224 ± 0.016 |
| Cacna1a ($Ca_V2.1$) | 0.022 ± 0.002 | 0.022 ± 0.001 | 0.023 ± 0.002 | 0.026 ± 0.003 |
| Cacna1g ($Ca_V3.1$) | 0.072 ± 0.007 | 0.030 ± 0.003 *** | 0.053 ± 0.006 | 0.038 ± 0.003 |
| Cacna1h ($Ca_V3.2$) | 0.151 ± 0.017 | 0.118 ± 0.013 | – | – |
| Trpc1 (TRPC1) | 0.100 ± 0.008 | 0.143 ± 0.011 | 0.110 ± 0.006 | 0.136 ± 0.009 |
| Trpc3 (TRPC3) | 0.078 ± 0.007 | 0.086 ± 0.011 | 0.061 ± 0.007 | 0.077 ± 0.009 |
| Trpc6 (TRPC6) | 0.131 ± 0.010 | 0.146 ± 0.013 | 0.163 ± 0.015 | 0.164 ± 0.013 |

***$P < 0.001$ in young *vs.* adult WT.

## Discussion

The present study addresses the putative role of $Ca_V3.2$ T-type $Ca^{2+}$ channels in vasomotor tone responses induced by changes in mechanical forces that are continuously acting on the vascular wall *in vivo*, such as flow (shear stress) and pressure (wall stress). We eliminated the potential influence of neurohormonal regulation using excised small resistance arteries, and we attempted to approximate physiological conditions using pressure myography with an *in vivo*-like temperature, $[CO_2/HCO_3^-]$ and pH. To avoid basing our conclusions on unspecific pharmacological T-type antagonists, such as mibefradil, NNC 55-0396 and $Ni^{2+}$ (Björling *et al.* 2013; Moosmang *et al.* 2006; Stockand *et al.* 1993;), we carried out a rigorous comparison of age-matched WT mice and mice with a global knockout of the Cacna1h gene encoding the $Ca_V3.2$ T-type $Ca^{2+}$ channels (Chen *et al.* 2003), which were previously found expressed at the mRNA (Braunstein *et al.* 2009; Gustafsson *et al.* 2001) and protein levels (Braunstein *et al.* 2009) in rat SMAs and arterioles. Because cardiovascular defects are often aggravated with advancing age, we compared all functional and structural responses in small arteries from young *vs.* mature adult mice of both genotypes.

First, we compared myogenic responsiveness in young *vs.* mature WT and $Ca_V3.2$KO mice. The WT arteries from young mice developed a MR at pressures >60 mmHg and this was significantly enhanced by 30 $\mu$M $Ni^{2+}$, which was previously shown to be more specific for inhibition of $Ca_V3.2$ over $Ca_V3.1$ and $Ca_V3.3$ currents (Lee *et al.* 1999). In young $Ca_V3.2$KO arteries, the active pressure-induced constriction was enhanced compared to WT, and no further effect was achieved by adding $Ni^{2+}$ (Figs 1*A* and *B*), showing that $Ni^{2+}$ interfered with the $Ca_V3.2$ channels. In mature adult WT arteries, the MR developed at pressures >40 mmHg, and there was no effect as a result of adding $Ni^{2+}$ in the WT. Furthermore, highly similar effects were obtained in the absence and presence of $Ni^{2+}$ in the mature adult $Ca_V3.2$KO arteries (Figs 1*C* and *D*). Taken together, our data suggest that $Ca_V3.2$ channels act as a vasodilator to oppose myogenic constriction in young mice (median age

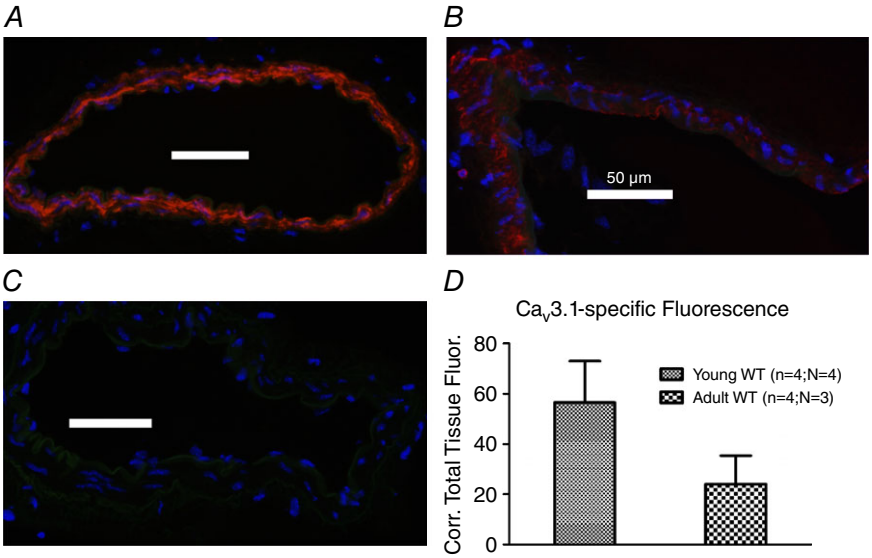


**Figure 8. Age-dependent intensity of $Ca_V3.1$-specific staining in mouse SMAs**
Immunostaining of the $Ca_V3.1$ T-type isoform (red colour) in young (*A*) *vs.* mature adult (*B*) WT mouse mesenteric arteries, and in staining without primary antibody (*C*). Note the lower fluorescence intensity visible in the mature adult artery compared to the young artery. Images were acquired using same settings of microscope, camera and software. Quantitation of background-corrected total tissue fluorescence in young *vs.* mature adult arteries using ImageJ (*D*).

of 12 weeks), although this effect vanishes in adult mice at a median age of 42 weeks, which, in humans, corresponds to between the mature adult and middle age (Flurkey *et al.* 2007). The lack of an effect of $Ca_V3.2$ deletion in mature adult mice could not be explained by a lower expression level of $Ca_V3.2$ channels because the transcript level of this channel was not significantly different in young and adult mouse mesenteric arteries (Table 3) and also because we did not observe an age-dependent difference in $Ca_V3.2$ immunofluorescence imaging experiments. This does not rule out the possibility that the channel function could be decreased in adult compared to young WT mice. The effect on MT observed in young mice is in agreement with several independent observations in the literature. First, the original study of $Ca_V3.2$KO mice performed by Chen *et al.* (2003) showed that $Ca_V3.2$KO mouse coronary arterioles were significantly more constricted than WT, and also that this was coincident with a higher prevalence of cardiac fibrosis. Second, recent studies have shown that MT in rodent and human cerebral arteries was enhanced by the addition of 50 $\mu$M $Ni^{2+}$ (Harraz *et al.* 2014*a*; Harraz *et al.* 2015*b*). Finally, a very recent study has duplicated our findings showing that MT was enhanced in SMAs from young (8–16 weeks) $Ca_V3.2$KO mice compared to WT (Harraz *et al.* 2015*a*). The latter study reported that 50 $\mu$M $Ni^{2+}$ suppressed $Ca^{2+}$ spark frequency and caused depolarization in VSMCs from the SMA of WT mice but not those from $Ca_V3.2$KO mice. However, the $Ca^{2+}$ spark frequency and resting membrane potential under control conditions were similar in SMAs from WT and $Ca_V3.2$KO mice. It would have been interesting to evaluate whether the resting cytosolic $Ca^{2+}$ concentration and/or the $Ca^{2+}$ sensitivity is increased in the $Ca_V3.2$KO mice because this would explain the increased MT that was observed. Because cardiac fibrosis was more prevalent in $Ca_V3.2$KO mice compared to WT, and because this effect was dramatically increased in 1-year-old mice (Chen *et al.* 2003), our data showing an age-dependent role of $Ca_V3.2$ channels in negative feedback on myogenic constriction could indicate a cardioprotective role of $Ca_V3.2$ channel expression in small resistance vessels in young individuals. This effect should not be confused with the reappearance of $Ca_V3.2$ channel expression in adult ventricular myocytes in mice with pressure overload-induced cardiac hypertrophy (Chiang *et al.* 2009). It is very intriguing that a previous study found young (8–10 weeks) $Ca_V3.2$KO mice to be normotensive and to demonstrate a normal heart rate compared to age-matched WT mice (Thuesen *et al.* 2014). With a higher basal tone at rest in the coronary, cerebral and mesenteric vasculature, the total peripheral resistance must be increased. Furthermore, with no indication of a lower sympathetic drive, the mean arterial pressure should be increased. We suggest that compensatory vasodilatation (e.g. by metabolic coupling) counteracts the increased basal tone in a major vascular bed such as the skeletal muscle. Alternatively, the cardiac stroke volume, which to our knowledge has not been measured in $Ca_V3.2$KO mice, is decreased, such that the mean arterial pressure is unchanged.

The proposed effect of 50 $\mu$M $Ni^{2+}$ with respect to enhancing MT via $Ca_V3.2$ inhibition, as shown in several recent studies (Harraz *et al.* 2014*a*; Harraz *et al.* 2015*a*; Harraz *et al.* 2015*b*), is consistent with the lack of an effect of 30 $\mu$M $Ni^{2+}$ in arteries from the $Ca_V3.2$KO mice in the present study. However, we also demonstrated that 30 $\mu$M $Ni^{2+}$ induced highly similar and significant acute vasoconstrictions in arteries maintained at 60 mmHg in both young and mature WT mice, as well as $Ca_V3.2$KO mice (Fig. 5). In addition, $Ni^{2+}$ inhibited endothelium-dependent vasodilatation to ACh in the $Ca_V3.2$KO mice (Fig. 4*A* and *B*), and there was a significant main effect of $Ni^{2+}$ with respect to inhibiting FMVD in all mice. Thus, the effects of $Ni^{2+}$, as used to extrapolate the significance of $Ca_V3.2$ channels in the vasculature in many previous studies, must be interpreted with caution because it is evident from the results of the present study that $Ni^{2+}$ bypasses $Ca_V3.2$ channels to promote vasoconstriction/inhibit vasodilatation via other mechanisms. It was previously shown that $BK_{Ca}$ channel currents were inhibited by $<1$ $\mu$M $Ni^{2+}$ in bovine mesenteric artery myocytes (Stockand *et al.* 1993) and this may partially explain the effects of $Ni^{2+}$ observed in WT and $Ca_V3.2$ KO mice in the present study. Nevertheless, these observations highlight the poor selectivity of T-type pharmacological tools and the need to employ knockout or knockdown studies to infer the function of T-type channels in the vasculature. As a result of the frequent use of T-type channel modulators, it is important to re-evaluate a proposed link between $Ca_V3.2$ channels and $BK_{Ca}$ channels and the negative modulation of myogenic constriction. This link was originally proposed as a result of the demonstration of a physical interaction between $Ca_V3.2/BK_{Ca}$ in mouse brain microsomes using co-immunoprecipitation (Chen *et al.* 2003). It was developed further as a model to explain negative feedback in the MR in cerebral arteries (Harraz *et al.* 2014*a*; Harraz *et al.* 2015*a*). We therefore tested the effect of $BK_{Ca}$ inhibition in VSMCs *in situ* using 1 $\mu$M paxilline (Li & Cheung, 1999) and found that MT was significantly enhanced by paxilline in young WT mice, and also that this effect was absent in $Ca_V3.2$KO arteries (Fig. 1*G* and *H*). Although this effect certainly argues for the relevance of a coupling between $Ca_V3.2/BK_{Ca}$ with respect to modifying MT development, it does not show the universal importance of this coupling because it must be absent in mature adult arteries in which we showed no role of $Ca_V3.2$ channels.

To further our understanding of the role of $Ca_V3.2$ channels in arteriolar tone regulation, we investigated both endothelium-dependent and independent vasodilator

mechanisms, with the primary focus being on FMVD. In rat SMAs, FMVD responses to a driving pressure ($\Delta P$) of 20 mmHg along the vessel were robust and reversible. Because FMVD responses were only insignificantly affected by L-Name (Fig. 2*B*), we tested the effect of $SK_{Ca}$ and $IK_{Ca}$ channel blockers. Indeed, the addition of a cocktail of 50 nM apamin + 1 $\mu$M Tram-34 strongly inhibited the FMVD (Fig. 2*C*), indicating that the EDH mechanism plays a prominent role in FMVD in this vascular bed. This observation is supported by a previous study showing that an EDH-like mechanism is involved in FMVD in SMAs (Takamura *et al.* 1999), whereas other studies have shown that it is most probably the $K_{Ca}2.3$ ($SK_{Ca}$) channels that are involved in the FMVD responses by being co-localized with shear stress-activated TRPV4 channels in endothelial submembranous $Ca^{2+}$ compartments, such as caveolae (Ma *et al.* 2013; Goedicke-Fritz *et al.* 2015). Because we found $Ca_V3.2$ to be expressed in EC in rat mesenteric arteries and arterioles (Braunstein *et al.* 2009), we hypothesized that $Ca_V3.2$ could be involved in activation of endothelial $K_{Ca}$ channels during FMVD; for example, by being co-localized with TRPV4/$SK_{Ca}$ in caveolae. Indeed, our first pharmacological observations using 100 $\mu$M $Ni^{2+}$ appeared to confirm that $Ca_V3.2$ channels were involved because the flow-mediated dilatation was reverted to a constriction by $Ni^{2+}$ (Fig. 2*D*). Thus, we tested the FMVD responses with and without $Ni^{2+}$ in young *vs.* mature adult WT and $Ca_V3.2$KO mice (Fig. 3*A*–*B*). However, $Ni^{2+}$ had no significant effects on the FMVD response in either of the mouse strains. It is therefore difficult to determine whether the effects of $Ni^{2+}$ on FMVD in rats were the result of blockade of $Ca_V3.2$ channels; however, the effects might be partially $Ca_V3.2$ independent because, in the young $Ca_V3.2$KO mice, we observed an apparent reversal of flow-induced dilatation to a constriction, and we also found a main effect of $Ni^{2+}$ to inhibit FMVD in all mice. Nevertheless, the most important observation from these experiments is that the FMVD response was significantly reduced (~50%) in young $Ca_V3.2$KO mice compared to age-matched WT mice, whereas no difference was observed for mature adult mice. This is very interesting because the age-dependency is similar to that observed for the MR (Fig. 1*A*–*F*), confirming our hypothesis that $Ca_V3.2$ channels are involved in either the sensing of shear stress or in the downstream signalling cascade to produce vasodilatation. There are no reports that $Ca_V3.2$ channels are mechano-sensitive *per se*, although they are required for normal D-hair receptor excitability and mechano-sensitivity in dorsal root ganglia in mice (Shin *et al.* 2003). Another possibility is that they might be stimulated by shear stress-evoked $Ca^{2+}$ entry into EC either through TRPV4 channels or $P2X_4$ receptors. Such stimulation of channel activity could arise if $Ca^{2+}$-dependent CamKII-kinase is allowed to phosphorylate $Ca_V3.2$ channels (Welsby *et al.*, 2003). Alternatively, the $Ca_V3.2$ channels are activated downstream of the shear stress-dependent production of vasodilators such as $PGI_2$, epoxyeicosatrienoic acids or hydrogen peroxide. Indeed, $PGI_2$ activates PKA, which was shown to augment $Ca_V3.2$ channel activity (Kim *et al.* 2006). Because these vasodilators can diffuse to the underlying VSMCs, the $Ca_V3.2$ channels localized in this cell layer could be indirectly involved in the FMVD responses. Our finding that $Ca_V3.2$ channels were strongly expressed in the VSMC layer but only weakly expressed in the endothelium (Fig. 7) may not be consistent with a primary role of endothelial $Ca_V3.2$ channels. In the present study, we cannot definitively clarify the mechanism responsible for how $Ca_V3.2$ is involved in flow responses, and this requires further dissection of the signalling mechanisms. ACh (10 $\mu$M) was used at the end of all the FMVD experiments to confirm the presence of an intact endothelium. There was no difference between WT and $Ca_V3.2$KO in either young or mature adult mice, although there was a highly similar and significant reduction of ACh dilatation by $Ni^{2+}$ in WT and $Ca_V3.2$KO mice, again showing that $Ni^{2+}$ has $Ca_V3.2$ independent effects in native vascular tissues (Figs 4*A* and *B*). Furthermore, endothelium independent vasodilatation to SNAP or as a result of raising extracellular [KCl] was not different between WT and $Ca_V3.2$KO mice, indicating the specific involvement of $Ca_V3.2$ in flow-induced responses (Figs 4*C*–*D*). This also allows exclusion of the effects of $Ca_V3.2$ via the cGMP/PKG pathway, as well as via $K_{ir}$ channel activation, because this would have affected our results using SNAP and raised extracellular [KCl], respectively.

By quantitating the mRNA expression profile in WT *vs.* $Ca_V3.2$KO mice (Table 3), we were able to rule out transcriptional changes in the expression of an array of important ion channels that could have compromised our conclusions. However, we did find a highly significant reduction in the transcript of the Cacna1g gene encoding the $Ca_V3.1$ T-type channel in mature adult mice compared to young WT mice. This age-dependent effect did not reach statistical significance in $Ca_V3.2$ KO mice. We found that the specific $Ca_V3.1$-fluorescence immunostaining was much weaker in vessels from mature adult WT mice (Fig. 8*A*–*C*) and, using a semi-quantitative image-based approach, we could detect a reduction in the corrected total tissue fluorescence intensity by >50% (Fig. 8*D*). In $Ca_V3.2$KO mice, we could not detect such age-dependent reduction of specific $Ca_V3.1$-fluorescence immunostaining. An age-related down-regulation of $Ca_V3.1$ mRNA and protein expression was previously demonstrated in the brains of humans and mice (Rice *et al.* 2014). This down-regulation of $Ca_V3.1$ protein might be considered to play a role

in the age-dependent effect of $Ca_V3.2$ channels in both MT and FMVD (e.g. by co-localization and/or functional linkage of $Ca_V3.1/Ca_V3.2$ in vascular cells). The $Ca_V3.1$ down-regulation coincides with the increased noradrenergic tone in mature adult WT arteries observed in the present study (Table 2). This could indicate a further role of $Ca_V3.1$ in vasodilatation, in addition to a role in MT at hyperpolarized voltages (Björling *et al.* 2013), and such a role in vasodilatation has been proposed previously (Svenningsen *et al.* 2014).

Using mice deficient in the $Ca_V3.2$ T-type $Ca^{2+}$ channel, we showed an age-dependent role of $Ca_V3.2$ in MT and FMVD, which was present only at a young age. With a dual role in myogenic and flow-induced tone regulation, $Ca_V3.2$ channels may have an important modulatory effect on blood pressure and flow-regulation in young individuals. We suggest that the function of $Ca_V3.2$ in small arteries at a young age offers a protective role against excess arterial tone and cardiovascular disease, which is lost with advancing age. Finally, our discovery of an age-dependent decline in mRNA and protein expression of the $Ca_V3.1$ T-type isoform indicates a general role of T-type channels in the process of ageing and perhaps in senescence in small arteries, which must be pursued in future studies.

## References


Ando J & Yamamoto K (2013). Flow detection and calcium signalling in vascular endothelial cells. *Cardiovasc Res* **99**, 260–268.

Ball CJ, Wilson DP, Turner SP, Saint DA & Beltrame JF (2009). Heterogeneity of L- and T-channels in the vasculature: rationale for the efficacy of combined L- and T-blockade. *Hypertension* **53**, 654–660.

Bhagyalakshmi A & Frangos JA (1989). Mechanism of shear-induced prostacyclin production in endothelial cells. *Biochem Biophys Res Commun* **158**, 31–37.

Bijlenga P, Liu JH, Espinos E, Haenggeli CA, Fischer-Lougheed J, Bader CR & Bernheim L (2000). T-type alpha 1H $Ca^{2+}$ channels are involved in Ca2+ signaling during terminal differentiation (fusion) of human myoblasts. *Proc Natl Acad Sci USA* **97**, 7627–7632.

Björling K, Morita H, Olsen MF, Prodan A, Hansen PB, Lory P, Holstein-Rathlou NH & Jensen LJ (2013). Myogenic tone is impaired at low arterial pressure in mice deficient in the low-voltage-activated CaV 3.1 T-type Ca(2+) channel. *Acta Physiol (Oxf)* **207**, 709–720.

Blanks AM, Zhao ZH, Shmygol A, Bru-Mercier G, Astle S & Thornton S (2007). Characterization of the molecular and electrophysiological properties of the T-type calcium channel in human myometrium. *J Physiol* **581**, 915–926.

Brahler S, Kaistha A, Schmidt VJ, Wolfle SE, Busch C, Kaistha BP, Kacik M, Hasenau AL, Grgic I, Si H, Bond CT, Adelman JP, Wulff H, de WC, Hoyer J & Kohler R (2009). Genetic deficit of SK3 and IK1 channels disrupts the endothelium-derived hyperpolarizing factor vasodilator pathway and causes hypertension. *Circulation* **119**, 2323–2332.

Brandes RP, Schmitz-Winnenthal FH, Feletou M, Godecke A, Huang PL, Vanhoutte PM, Fleming I & Busse R (2000). An endothelium-derived hyperpolarizing factor distinct from NO and prostacyclin is a major endothelium-dependent vasodilator in resistance vessels of wild-type and endothelial NO synthase knockout mice. *Proc Natl Acad Sci USA* **97**, 9747–9752.

Braunstein TH, Inoue R, Cribbs L, Oike M, Ito Y, Holstein-Rathlou NH & Jensen LJ (2009). The role of L- and T-type channels in local and remote calcium responses in rat mesenteric terminal arterioles. *J Vasc Res* **46**, 138–151.

Brueggemann LI, Martin BL, Barakat J, Byron KL, & Cribbs LL (2005). Low voltage-activated calcium channels in vascular smooth muscle: T-type channels and AVP-stimulated calcium spiking. *Am J Physiol Heart Circ Physiol* **288**, H923–H935.

Bubolz AH, Mendoza SA, Zheng X, Zinkevich NS, Li R, Gutterman DD & Zhang DX (2012). Activation of endothelial TRPV4 channels mediates flow-induced dilation in human coronary arterioles: role of $Ca^{2+}$ entry and mitochondrial ROS signaling. *Am J Physiol Heart Circ Physiol* **302**, H634–H642.

Chemin J, Monteil A, Bourinet E, Nargeot J & Lory P (2001). Alternatively spliced alpha(1 G) (Ca(V)3.1) intracellular loops promote specific T-type Ca(2+) channel gating properties. *Biophys J* **80**, 1238–1250.

Chen CC, Lamping KG, Nuno DW, Barresi R, Prouty SJ, Lavoie JL, Cribbs LL, England SK, Sigmund CD, Weiss RM, Williamson RA, Hill JA & Campbell KP (2003). Abnormal coronary function in mice deficient in alpha1H T-type $Ca^{2+}$ channels. *Science* **302**, 1416–1418.

Chiang CS, Huang CH, Chieng H, Chang YT, Chang D, Chen JJ, Chen YC, Chen YH, Shin HS, Campbell KP & Chen CC (2009). The Ca(v)3.2 T-type Ca(2+) channel is required for pressure overload-induced cardiac hypertrophy in mice. *Circ Res* **104**, 522–530.

Christensen FH, Hansen T, Stankevicius E, Buus NH & Simonsen U (2007). Elevated pressure selectively blunts flow-evoked vasodilatation in rat mesenteric small arteries. *Br J Pharmacol* **150**, 80–87.

Cribbs LL (2006). T-type $Ca^{2+}$ channels in vascular smooth muscle: multiple functions. *Cell Calcium* **40**, 221–230.

Dora KA, Gallagher NT, McNeish A & Garland CJ (2008). Modulation of endothelial cell KCa3.1 channels during endothelium-derived hyperpolarizing factor signaling in mesenteric resistance arteries. *Circ Res* **102**, 1247–1255.

Dora KA, Hinton JM, Walker SD & Garland CJ (2000). An indirect influence of phenylephrine on the release of endothelium-derived vasodilators in rat small mesenteric artery. *Br J Pharmacol* **129**, 381–387.

Edwards G, Dora KA, Gardener MJ, Garland CJ & Weston AH (1998). $K^+$ is an endothelium-derived hyperpolarizing factor in rat arteries. *Nature* **396**, 269–272.

Emerick MC, Stein R, Kunze R, McNulty MM, Regan MR, Hanck DA & Agnew WS (2006). Profiling the array of Ca(v)3.1 variants from the human T-type calcium channel gene CACNA1G: alternative structures, developmental expression, and biophysical variations. *Proteins* **64**, 320–342.

Fleming I & Busse R (1999). Signal transduction of eNOS activation. *Cardiovasc Res* **43**, 532–541.

Flurkey K, Currer JM, & Harteneck C (2007). Mouse Models in Aging Research. In *The Mouse in Biomedical Research: Normative Biology, Husbandry, and Models*, eds J. G. Fox, S. W. Barthold, M. T. Davisson, C. E. Newcomer, F. W. Quimby & A. L. Smith, pp. 637–672. Academic Press, Burlington, MA.

Goedicke-Fritz S, Kaistha A, Kacik M, Markert S, Hofmeister A, Busch C, Banfer S, Jacob R, Grgic I & Hoyer J (2015). Evidence for functional and dynamic microcompartmentation of Cav-1/TRPV4/K in caveolae of endothelial cells. *Eur J Cell Biol* **94**, 391–400.

Gustafsson F, Andreasen D, Salomonsson M, Jensen BL & Holstein-Rathlou N (2001). Conducted vasoconstriction in rat mesenteric arterioles: role for dihydropyridine-insensitive Ca(2+) channels. *Am J Physiol Heart Circ Physiol* **280**, H582–H590.

Harraz OF, Abd El-Rahman RR, Bigdely-Shamloo K, Wilson SM, Brett SE, Romero M, Gonzales AL, Earley S, Vigmond EJ, Nygren A, Menon BK, Mufti RE, Watson T, Starreveld Y, Furstenhaupt T, Muellerleile PR, Kurjiaka DT, Kyle BD, Braun AP & Welsh DG (2014*a*). Ca(V)3.2 channels and the induction of negative feedback in cerebral arteries. *Circ Res* **115**, 650–661.

Harraz OF, Brett SE & Welsh DG (2014*b*). Nitric oxide suppresses vascular voltage-gated T-type $Ca^{2+}$ channels through cGMP/PKG signaling. *Am J Physiol Heart Circ Physiol* **306**, H279–H285.

Harraz OF, Brett SE, Zechariah A, Romero M, Puglisi JL, Wilson SM & Welsh DG (2015*a*). Genetic ablation of CaV3.2 channels enhances the arterial myogenic response by modulating the RyR-BKCa axis. *Arterioscler Thromb Vasc Biol* **35**, 1843–1851.

Harraz OF, Visser F, Brett SE, Goldman D, Zechariah A, Hashad AM, Menon BK, Watson T, Starreveld Y & Welsh DG (2015*b*). CaV1.2/CaV3.x channels mediate divergent vasomotor responses in human cerebral arteries. *J Gen Physiol* **145**, 405–418.

Hill MA & Meininger GA (2012). Arteriolar vascular smooth muscle cells: mechanotransducers in a complex environment. *Int J Biochem Cell Biol* **44**, 1505–1510.

Hill MA, Meininger GA, Davis MJ & Laher I (2009). Therapeutic potential of pharmacologically targeting arteriolar myogenic tone. *Trends Pharmacol Sci* **30**, 363–374.

Huang A, Sun D, Jacobson A, Carroll MA, Falck JR & Kaley G (2005). Epoxyeicosatrienoic acids are released to mediate shear stress-dependent hyperpolarization of arteriolar smooth muscle. *Circ Res* **96**, 376–383.

Jensen LJ & Holstein-Rathlou NH (2009). Is there a role for T-type $Ca^{2+}$ channels in regulation of vasomotor tone in mesenteric arterioles? *Can J Physiol Pharmacol* **87**, 8–20.

Jensen LJ, Salomonsson M, Jensen BL & Holstein-Rathlou NH (2004). Depolarization-induced calcium influx in rat mesenteric small arterioles is mediated exclusively via mibefradil-sensitive calcium channels. *Br J Pharmacol* **142**, 709–718.

Kim JA, Park JY, Kang HW, Huh SU, Jeong SW & Lee JH (2006). Augmentation of Cav3.2 T-type calcium channel activity by cAMP-dependent protein kinase A. *J Pharmacol Exp Ther* **318**, 230–237.

Kohler R, Heyken WT, Heinau P, Schubert R, Si H, Kacik M, Busch C, Grgic I, Maier T & Hoyer J (2006). Evidence for a functional role of endothelial transient receptor potential V4 in shear stress-induced vasodilatation. *Arterioscler Thromb Vasc Biol* **26**, 1495–1502.

Koller A, Sun D & Kaley G (1993). Role of shear stress and endothelial prostaglandins in flow- and viscosity-induced dilation of arterioles in vitro. *Circ Res* **72**, 1276–1284.

Kuo IY, Ellis A, Seymour VA, Sandow SL & Hill CE (2010). Dihydropyridine-insensitive calcium currents contribute to function of small cerebral arteries. *J Cereb Blood Flow Metab* **30**, 1226–1239.

Kuo IY, Howitt L, Sandow SL, McFarlane A, Hansen PB & Hill CE (2014). Role of T-type channels in vasomotor function: team player or chameleon? *Pflügers Arch* **466**, 767–779.

Lee JH, Gomora JC, Cribbs LL & Perez-Reyes E (1999). Nickel block of three cloned T-type calcium channels: low concentrations selectively block alpha1H. *Biophys J* **77**, 3034–3042.

Li G & Cheung DW (1999). Effects of paxilline on K+ channels in rat mesenteric arterial cells. *Eur J Pharmacol* **372**, 103–107.

Liu Y, Bubolz AH, Mendoza S, Zhang DX & Gutterman DD (2011). $H_2O_2$ is the transferrable factor mediating flow-induced dilation in human coronary arterioles. *Circ Res* **108**, 566–573.

Ma X, Du J, Zhang P, Deng J, Liu J, Lam FF, Li RA, Huang Y, Jin J & Yao X (2013). Functional role of TRPV4-KCa2.3 signaling in vascular endothelial cells in normal and streptozotocin-induced diabetic rats. *Hypertension* **62**, 134–139.

Mendoza SA, Fang J, Gutterman DD, Wilcox DA, Bubolz AH, Li R, Suzuki M & Zhang DX (2010). TRPV4-mediated endothelial $Ca^{2+}$ influx and vasodilation in response to shear stress. *Am J Physiol Heart Circ Physiol* **298**, H466–H476.

Miura H, Wachtel RE, Liu Y, Loberiza FR, Jr., Saito T, Miura M & Gutterman DD (2001). Flow-induced dilation of human coronary arterioles: important role of Ca(2+)-activated K(+) channels. *Circulation* **103**, 1992–1998.

Moosmang S, Haider N, Bruderl B, Welling A & Hofmann F (2006). Antihypertensive effects of the putative T-type calcium channel antagonist mibefradil are mediated by the L-type calcium channel Cav1.2. *Circ Res* **98**, 105–110.

Moosmang S, Schulla V, Welling A, Feil R, Feil S, Wegener JW, Hofmann F & Klugbauer N (2003). Dominant role of smooth muscle L-type calcium channel Cav1.2 for blood pressure regulation. *EMBO J* **22**, 6027–6034.

Nelson MT, Patlak JB, Worley JF & Standen NB (1990). Calcium channels, potassium channels, and voltage dependence of arterial smooth muscle tone. *Am J Physiol Cell Physiol* **259**, C3–C18.

Nilius B & Droogmans G (2001). Ion channels and their functional role in vascular endothelium. *Physiol Rev* **81**, 1415–1459.

Parkington HC, Chow JA, Evans RG, Coleman HA & Tare M (2002). Role for endothelium-derived hyperpolarizing factor in vascular tone in rat mesenteric and hindlimb circulations in vivo. *J Physiol* **542**, 929–937.

Perez-Reyes E (2003). Molecular physiology of low-voltage-activated t-type calcium channels. *Physiol Rev* **83**, 117–161.

Potocnik SJ, McSherry I, Ding H, Murphy TV, Kotecha N, Dora KA, Yuill KH, Triggle CR & Hill MA (2009). Endothelium-dependent vasodilation in myogenically active mouse skeletal muscle arterioles: role of EDH and K(+) channels. *Microcirculation* **16**, 377–390.

Poulsen CB, Al-Mashhadi RH, Cribbs LL, Skott O & Hansen PB (2011). T-type voltage-gated calcium channels regulate the tone of mouse efferent arterioles. *Kidney Int* **79**, 443–451.

Qiu W, Kass DA, Hu Q & Ziegelstein RC (2001). Determinants of shear stress-stimulated endothelial nitric oxide production assessed in real-time by 4,5-diaminofluorescein fluorescence. *Biochem Biophys Res Commun* **286**, 328–335.

Rice RA, Berchtold NC, Cotman CW & Green KN (2014). Age-related downregulation of the CaV3.1 T-type calcium channel as a mediator of amyloid beta production. *Neurobiol Aging* **35**, 1002–1011.

Scotland RS, Madhani M, Chauhan S, Moncada S, Andresen J, Nilsson H, Hobbs AJ & Ahluwalia A (2005). Investigation of vascular responses in endothelial nitric oxide synthase/cyclooxygenase-1 double-knockout mice: key role for endothelium-derived hyperpolarizing factor in the regulation of blood pressure in vivo. *Circulation* **111**, 796–803.

Shimokawa H, Yasutake H, Fujii K, Owada MK, Nakaike R, Fukumoto Y, Takayanagi T, Nagao T, Egashira K, Fujishima M & Takeshita A (1996). The importance of the hyperpolarizing mechanism increases as the vessel size decreases in endothelium-dependent relaxations in rat mesenteric circulation. *J Cardiovasc Pharmacol* **28**, 703–711.

Shin JB, Martinez-Salgado C, Heppenstall PA & Lewin GR (2003). A T-type calcium channel required for normal function of a mammalian mechanoreceptor. *Nat Neurosci* **6**, 724–730.

Si H, Heyken WT, Wolfle SE, Tysiac M, Schubert R, Grgic I, Vilianovich L, Giebing G, Maier T, Gross V, Bader M, de WC, Hoyer J & Kohler R (2006). Impaired endothelium-derived hyperpolarizing factor-mediated dilations and increased blood pressure in mice deficient of the intermediate-conductance $Ca^{2+}$-activated $K^+$ channel. *Circ Res* **99**, 537–544.

Smirnov SV & Aaronson PI (1992). $Ca^{2+}$ currents in single myocytes from human mesenteric arteries: evidence for a physiological role of L-type channels. *J Physiol* **457**, 455–475.

Smirnov SV, Loutzenhiser K & Loutzenhiser R (2013). Voltage-activated Ca(2+) channels in rat renal afferent and efferent myocytes: no evidence for the T-type Ca(2+) current. *Cardiovasc Res* **97**, 293–301.

Socha MJ & Segal SS (2013). Isolation of microvascular endothelial tubes from mouse resistance arteries. *J Vis Exp* e50759.

Stockand J, Sultan A, Molony D, DuBose T, Jr. & Sansom S (1993). Interactions of cadmium and nickel with K channels of vascular smooth muscle. *Toxicol Appl Pharmacol* **121**, 30–35.

Svenningsen P, Andersen K, Thuesen AD, Shin HS, Vanhoutte PM, Skott O, Jensen BL, Hill C & Hansen PB (2014). T-type Ca(2+) channels facilitate NO-formation, vasodilatation and NO-mediated modulation of blood pressure. *Pflügers Arch* **466**, 2205–2214.

Takamura Y, Shimokawa H, Zhao H, Igarashi H, Egashira K & Takeshita A (1999). Important role of endothelium-derived hyperpolarizing factor in shear stress–induced endothelium-dependent relaxations in the rat mesenteric artery. *J Cardiovasc Pharmacol* **34**, 381–387.

Thorsgaard M, Lopez V, Buus NH & Simonsen U (2003). Different modulation by $Ca^{2+}$-activated $K^+$ channel blockers and herbimycin of acetylcholine- and flow-evoked vasodilatation in rat mesenteric small arteries. *Br J Pharmacol* **138**, 1562–1570.

Thuesen AD, Andersen H, Cardel M, Toft A, Walter S, Marcussen N, Jensen BL, Bie P & Hansen PB (2014). Differential effect of T-type voltage-gated $Ca^{2+}$ channel disruption on renal plasma flow and glomerular filtration rate in vivo. *Am J Physiol Renal Physiol* **307**, F445–F452.

Walsh MP & Cole WC (2013). The role of actin filament dynamics in the myogenic response of cerebral resistance arteries. *J Cereb Blood Flow Metab* **33**, 1–12.

Welsby PJ, Wang H, Wolfe JT, Colbran RJ, Johnson ML & Barrett PQ (2003). A mechanism for the direct regulation of T-type calcium channels by $Ca^{2+}$/calmodulin-dependent kinase II. *J Neurosci* **23**, 10116–10121.

Yamamoto K, Korenaga R, Kamiya A & Ando J (2000). Fluid shear stress activates Ca(2+) influx into human endothelial cells via P2×4 purinoceptors. *Circ Res* **87**, 385–391.

## Additional information

### Competing interests

The authors declare that they have no competing interests.

### Funding

The present study receieved support from The Danish Council for Independent Research | Medical Sciences, The Novo Nordisk Foundation, The Danish Heart Foundation and The A.P. Møller Foundation for the Advancement of Medical Science.

### Author contributions

MFM, KB and LJJ carried out conceptual design of the study and performed experiments. LJJ carried out breeding of knockout mice and secured funding for the project. MFM, KB, and LJJ drafted the final version of the manuscript. All authors have approved the final version of the manuscript and agree to be accountable for all aspects of the work. All persons designated as authors qualify for authorship, and all those who qualify for authorship are listed.

### Acknowledgements

Vibeke Grøsfjeld Christensen is gratefully acknowledged for providing expert technical assistance. Professor Pernille B. L. Hansen is gratefully acknowledged for providing the $Ca_V3.2$ knockout mice used in the study, as well as for reading the manuscript. We also thank Professor Niels-Henrik Holstein-Rathlou for carefully reading the manuscript.